

## TAILORING SPECTROSCOPIC PROPERTIES OF ER<sup>3+</sup> DOPED ZINC SODIUM TELLURITE GLASS VIA GOLD NANOPARTICLES

Asmahani Awang<sup>a</sup>, S.K. Ghoshal<sup>b\*</sup>, M.R. Sahar<sup>b</sup>, R. Arifin<sup>b</sup>

<sup>a</sup>Physics with Electronics Program, Faculty of Science and Natural Resources, Universiti Malaysia Sabah, 88400 Kota Kinabalu, Sabah, Malaysia.

<sup>b</sup>Advanced Optical Materials Research Group, Department of Physics, Faculty of Science, Universiti Teknologi Malaysia, 81310 UTM Johor Bahru, Johor, Malaysia.

### Article history

Received

10 February 2015

Received in revised form

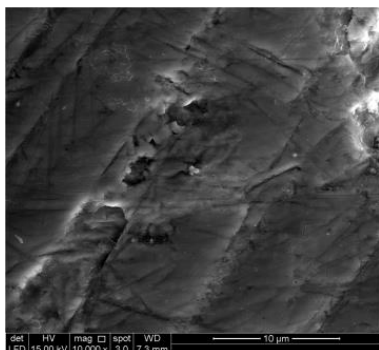
10 November 2015

Accepted

12 November 2015

\*Corresponding author  
sibkrishna@utm.my

### Graphical abstract



### Abstract

Tailoring the spectroscopic properties of rare earth (RE) doped inorganic glasses mediated via surface plasmon resonance (SPR) by embedding metallic nanoparticles (NPs) with controlled concentration is prerequisite for photonic applications. Erbium (Er<sup>3+</sup>) doped tellurite glasses containing gold (Au) NPs are prepared and systematic characterizations are made to inspect the impacts of Au NPs of spectral features for desired tailoring. X-ray diffraction pattern confirm the amorphous nature of the glass samples and EDX analysis detects elemental traces. The UV-Vis spectra exhibit six absorption bands centered at 488, 523, 655, 800, 973 and 1533 nm corresponding to 4f-4f transitions of Er<sup>3+</sup> ions. Glass sample containing 0.4 mol% Au (without Er<sub>2</sub>O<sub>3</sub>) reveals Au plasmon band at around 629 nm. The EDX spectra display elemental traces of Te, Er, Zn, Na and Au. Glass sample containing 0.2 mol% Au demonstrates maximum enhancement in the emission band intensity by a factor of 20.23 (orange), 18.35 (strong green), 16.80 (moderate green) and 15.46 (blue). The enhancement is attributed to the Au NPs assisted SPR effect. The beneficial features of proposed glasses nominate them as potential candidate for photonic devices and solid state lasers.

Keywords: Glasses; SPR; nanoparticles; amorphous

### Abstrak

Pengubahan sifat spektroskopi gelas tak organik didopkan dengan nadir bumi (RE) dirangsang melalui resonans plasmon permukaan (SPR) dengan memasukkan nanozarah (NPs) logam dengan kawalan kepekatan adalah penting bagi aplikasi fotonik. Gelas telurit didopkan dengan erbium (Er<sup>3+</sup>) mengandungi NPs emas (Au) telah disediakan dan pencirian sistematik telah dibuat untuk mengesahkan kesan NPs Au terhadap sifat spektrum untuk mendapatkan ciri pengubahsuaian yang diinginkan. Pola pembelauan sinar-X membuktikan sifat amorfus sampel gelas dan analisis EDX mengesan unsur yang hadir. Spektra UV-Vis menunjukkan enam jalur serapan berpusat pada 488, 523, 655, 800, 973 dan 1533 nm merujuk pada peralihan 4f-4f bagi ion-ion Er<sup>3+</sup>. Sampel gelas yang mengandungi 0.4 mol% Au (tanpa Er<sub>2</sub>O<sub>3</sub>) menunjukkan jalur plasmon Au di sekitar 629 nm. Spektra EDX menunjukkan kesan unsur bagi Te, Er, Zn, Na dan Au. Sampel gelas yang mengandungi 0.2 mol% Au menunjukkan peningkatan maksimum pada jalur serapan dengan gandaan sebanyak 20.23 (jingga), 18.35 (hijau yang kuat), 16.80 (hijau yang sederhana) and 15.46 (biru). Peningkatan dikaitkan pada NPs Au memangkin kesan SPR. Ciri-ciri

bermanfaat gelas yang dicadangkan mencalonkan gelas tersebut berpotensi bagi peralatan fotonik dan laser keadaan pepejal.

*Kata kunci:* Gelas; SPR; nanozarah; amorfus

© 2016 Penerbit UTM Press. All rights reserved

## 1.0 INTRODUCTION

Tellurite glasses has an advantages over other host glass due to their relative low-phonon energy ( $\approx 700 \text{ cm}^{-1}$ ), high refractive index values ( $\approx 2.0$ ), high dielectric constant, good corrosion resistance, large transmittance window in the visible and near infrared region, high solubility of rare-earth (RE) ions, thermal and chemical stability.<sup>1,2</sup> In addition, they possess relatively low transformation temperatures, high densities and non hygroscopic properties.<sup>3</sup> Trivalent RE ions doped  $\text{TeO}_2$ -based glasses presenting large luminescence efficiency in various wavelengths ranges are considered to be highly useful host materials.<sup>4</sup> Tellurite glasses containing high concentrations RE ions are attractive for optical data transmission, detection, sensing, and laser technologies.<sup>5</sup> Recently, RE ions coupled with plasmonic nanoclusters have been

developed to enhance the luminescence intensity of RE ions.

Plasmonic metal NPs have an ability to confine the electromagnetic energy or optical excitation in a nanoscale volume to mediate strong optical interactions by local electric field enhancements.<sup>6,7</sup> However, positioning the metallic NPs of desired sizes and shapes in the vicinity of RE ions is the greatest challenge.<sup>8,9</sup> Despite much effort, the mechanism behind the interaction of metallic NPs with RE ions in the glass matrix in improving the spectroscopic properties are still lacking. Accordingly, we incorporate Au NPs into the tellurite glass matrix to examine the interaction between metal nanoclusters with  $\text{Er}^{3+}$  ions for possible tailoring. Present study inspects the spectroscopic properties of these glasses which are remarkably modified via optimized concentration by tuning the concentration of Au NPs. We examine the effect of SPR on the enhancement of luminescence intensity of erbium-zinc-sodium-tellurite glass containing Au NPs.

**Table 1** The glass composition (mol%) of respective glass samples

Glass	$\text{TeO}_2$	$\text{ZnO}$	$\text{Na}_2\text{O}$	$\text{Er}_2\text{O}_3$	<b>Au</b>
S1	70	20	10	0.5	0
S2	70	20	10	0.5	0.2
S3	70	20	10	0.5	0.4
S4	70	20	10	-	-
S5	70	20	10	-	0.4

## 2.0 EXPERIMENTAL

Glass samples with composition  $70\text{TeO}_2\text{-}20\text{ZnO-}10\text{Na}_2\text{O-(x)Er}_2\text{O}_3\text{-(y)Au}$  ( $x = 0.0$  and  $0.5$  mol%;  $y = 0.0$ ,  $0.2$  and  $0.4$  mol% in excess) are synthesized using melt-quenching technique as shown in Table 1. Starting materials of  $\text{TeO}_2$ ,  $\text{ZnO}$ ,  $\text{Na}_2\text{O}$ ,  $\text{Er}_2\text{O}_3$  and Au from Sigma Aldrich with 99.9% purity are mixed thoroughly. A platinum crucible containing the glass constituents is placed in a furnace at  $900^\circ\text{C}$  for 25 min and melted before placing the melt in a brass mould. Subsequently, the sample was transferred to an annealing furnace and kept for 3 h at  $295^\circ\text{C}$  to remove the thermal and mechanical strains. The samples are then cooled down to room temperature before cutting and polishing. Finally, the structural and optical measurements are performed.

The amorphous nature of glass is examined by Bruker D8 Advance XRD diffractometer using Cu K $\alpha$  radiations ( $\lambda = 1.54 \text{ \AA}$ ). The room temperature absorption spectra are recorded by using Shimadzu UV-3101PC scanning spectrophotometer (Kyoto,

Japan). The existence of Au NPs is identified by using FESEM Carl Zeiss Leo Supra 50VP. The excitation and emission spectra are recorded by a Perkin Elmer LS-55 photoluminescence (PL) spectrometer (UK) spectrometer.

## 3.0 RESULTS AND DISCUSSION

Figure 1 displays the typical XRD pattern of the glass sample without Au NPs. The presence of a broad hump between  $25\text{-}35^\circ$  without any sharp crystallization peaks confirms the amorphous nature of the sample.<sup>10</sup> The XRD pattern of all samples (not shown here) are nearly the same. The absence of sharp, strongly diffracted beams in the X-ray diffraction pattern from glass indicates that there are no well defined planes in the structure on or around which the constituent atoms are regularly arranged.<sup>3</sup>

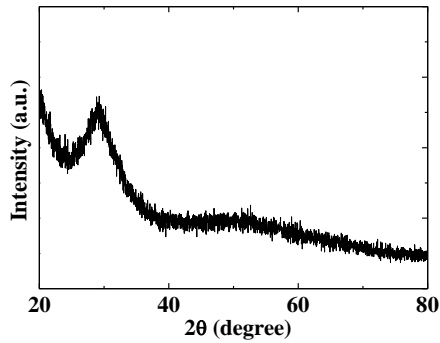


Figure 1 XRD pattern of glass sample without Au NPs

Figure 2(a) shows the room temperature UV-Vis-NIR absorption spectra of  $\text{Er}_2\text{O}_3$  doped glasses. Six absorption bands centered at 488, 523, 655, 800, 973 and 1533 nm corresponding to the transitions from the ground state  $4I_{15/2}$  of  $\text{Er}^{3+}$  ions to  $4F_{7/2}$ ,  $2H_{11/2}$ ,  $4F_{9/2}$ ,  $4I_{9/2}$ ,  $4I_{11/2}$  and  $4I_{13/2}$  excited states, respectively are observed. The appearance of a weak absorption band at 550 nm is assigned to  $4I_{15/2} \rightarrow 4S_{3/2}$  transition. The enhanced absorbance with the addition of Au content signifies role of Au NPs in the host matrix modification.<sup>10</sup> Dimitrova *et al.*,<sup>11</sup> acknowledged the metallic NPs concentration and composition dependent alteration in the absorption spectra (intensity of the absorption peak) of glass. In the current study, the observed significant increase in the absorption intensity for glass with varying Au content is primarily ascribed to the modification of glass network structures or the ligand field<sup>12</sup> around Au NPs. However, samples containing both Au NPs and  $\text{Er}^{3+}$  ions (co-doped samples) do not reveal any plasmon band due to the overshadowing effect of dominant  $\text{Er}^{3+}$  peaks.<sup>8</sup>

To probe the existence of Au Plasmon band, a glass sample with 0.4 mol% Au and without  $\text{Er}_2\text{O}_3$  is prepared. Figure 2(b) shows the vivid evidence of plasmon peak for gold NPs at around 629 nm. This clear emergence of intensive SPR absorption band in the UV-Vis spectrum confirms the existence of nanosized Au particles in the glass matrix. The strong absorption band represents the occurrence of fine metallic particles in a dielectric medium.<sup>13</sup>

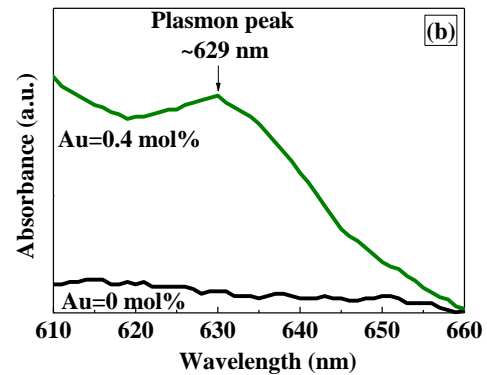
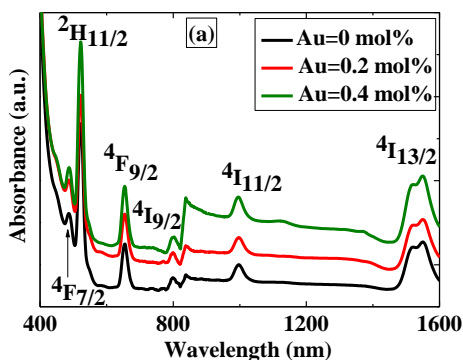
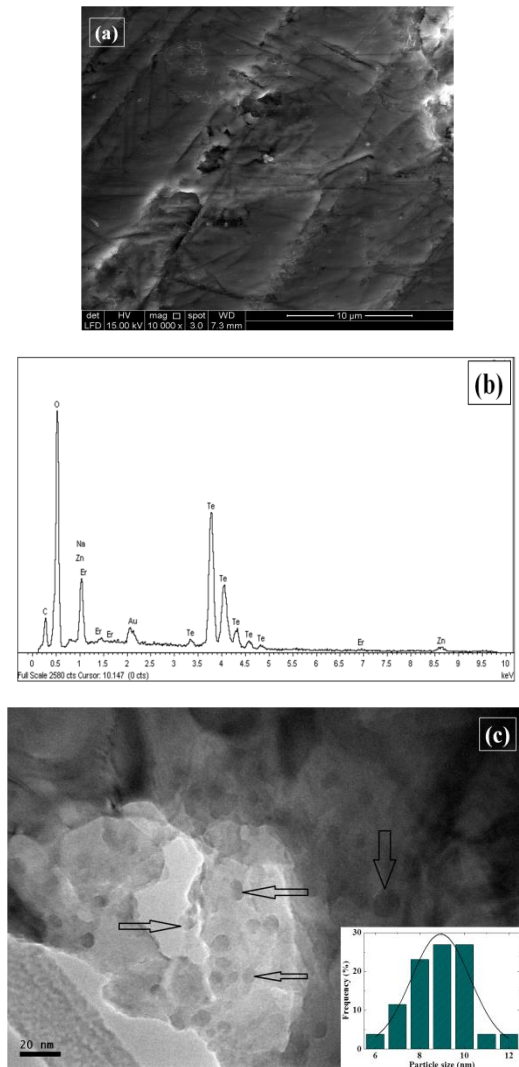


Figure 2 (a) UV-Vis-NIR absorption spectra of glass samples in the range of 400–1600 nm; (b) SPR band positions of gold NPs

Figure 3(a) represents the FESEM image of glass sample containing 0.4 mol% Au with nanosized probe for selected spots that directly identifies the existence and distribution of gold NPs. The examined particles illustrate the distribution of smaller objects range from 0.5  $\mu\text{m}$  to larger one of few micrometers in size. Nonetheless, the detailed structures of NPs cannot be observed due to the limitations of higher magnification. The wash out of the details on FESEM picture is resulted from sample charging effects.<sup>14</sup> The effect of charging leads to a degraded image and poor resolution. It also renders poor EDX analysis is caused by the incident beam being repelled from the investigated region. Therefore, the charging effects were avoided or minimized for non-conducting materials by coating the sample with a thin conductive layer such as gold, carbon, platinum or gold-palladium.<sup>15</sup>

The EDX spectrum provides information of the elemental traces in the glass matrix surrounding. The appearance of various peaks in the typical selected area EDX spectrum of glass (Figure 3(b)) exhibits the traces Te, Er, Zn, Na, and Au elements in the glass matrix. The intense peak located at 0.5 keV is related to the domination of oxygen (O). The incidence of carbon (C) peak is due to the coating material based vacuum-evaporated carbon. Generally, samples are often electrically non-conducting and a conducting surface coating must be applied to provide a path for the incident electrons to flow to ground.

For clear observation, Figure 3(c) shows the TEM image of the glass sample containing 0.4 mol% Au. Small Au NPs (show by black spots) majority with different sizes in non-spherical shape are visible dispersed in the glass matrix. Inset shows the size distribution of Au NPs in the same glass with Gaussian fits and average size about 9 nm.



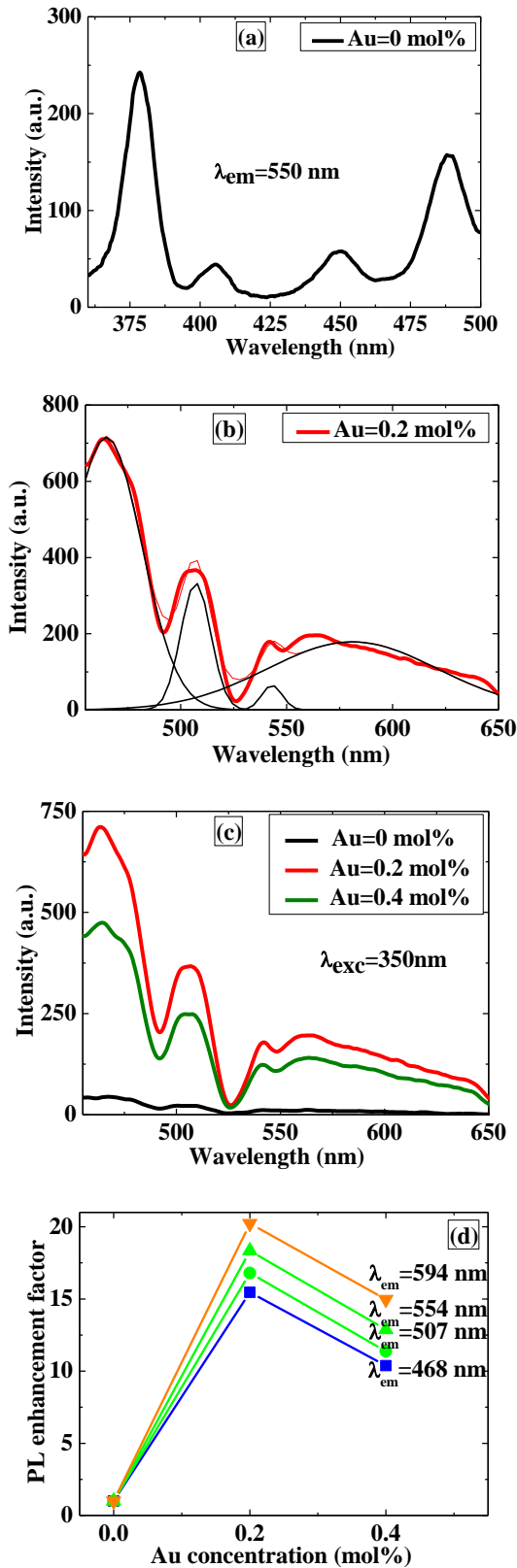
**Figure 3** (a) FESEM image at specific region of glass sample containing 0.4 mol% Au; (b) the respective EDX spectra of glass sample; (c) TEM image of the Au NPs (glass containing 0.4 mol% Au) show closely dispersed particles, majority with non-spherical shape. Inset shows histogram of Au NPs with average diameter of  $\approx 9$  nm

Figure 4(a) depicts the room temperature excitation spectra of  $\text{Er}^{3+}$ -doped glass (without Au NPs) in the wavelength range of 360–500 nm. Four transitions associated to  $^4\text{G}_{11/2}$ ,  $^2\text{H}_{9/2}$ ,  $^4\text{F}_{5/2}$  and  $^4\text{F}_{7/2}$  levels with the corresponding band position centered at 377, 406, 449 and 487 nm are evidenced. Furthermore, the transition of  $^4\text{G}_{11/2}$  at 375 nm shows the maximum intensity. The excitation around 350 nm

gives the finest PL spectra if to be compared with excitation at other wavelengths (not shown in figure). Accordingly, the wavelength at around 350 nm ( $^4\text{G}_{11/2}$  transition) is used as the excitation wavelength to investigate the PL spectra.

Figure 4(b) shows the fluorescence spectra of  $\text{Er}^{3+}$ -doped zinc sodium tellurite glass containing 0.2 mol% Au with de-convoluted Gaussian peaks. Figure 4(c) displays the emission spectra (with 350 nm excitations) for glass samples without and with Au NPs. The fluorescence spectra of  $\text{Er}^{3+}$  ion exhibit four peaks centered at 468, 507, 554 and 594 nm corresponding to  $^4\text{F}_{5/2} \rightarrow ^4\text{I}_{15/2}$ ,  $^4\text{F}_{7/2} \rightarrow ^4\text{I}_{15/2}$ ,  $^4\text{S}_{3/2} \rightarrow ^4\text{I}_{15/2}$  and  $^4\text{F}_{9/2} \rightarrow ^4\text{I}_{15/2}$  transitions, respectively. The emissions corresponding to the peaks centered at 468, 507, 554 and 594 nm for glass containing 0.2 mol% Au are found to be enhanced by a factor of 15.46, 16.80, 18.35 and 20.23 times (refer to Table 2), respectively. The achieved significant enhancements in the PL intensity are ascribed to the surface plasmon (SP) mediated contribution of Au NPs. However, further increase in Au concentration up to 0.4 mol% quenched the luminescence intensity. The existence of emission spectra around 450 nm and 451 nm (blue region) have been reported by Obadina *et al.*,<sup>16</sup> and Selvaraju *et al.*,<sup>17</sup> However, peak at 592 nm ( $^4\text{F}_{9/2} \rightarrow ^4\text{I}_{15/2}$ ) is rarely observed in oxide glass. In current study, addition of Au NPs as shown in Figure 4(c) has increased the luminescence intensities considerably. This behavior may be due to intermixing of electronic level of  $\text{Er}^{3+}$  with molecular orbital of dopants<sup>18</sup> (Au NPs) resulting in the increase in the population of the excited states of  $\text{Er}^{3+}$ . However, the associated mechanism is beyond of our study.

Figure 4(d) displays the PL enhancement factor for observed bands as listed in Table 2. The enhancement is found to be highest for emission at around 594 nm for glass containing 0.2 mol% Au. The higher enhancement for emission at around 594 nm is attributed to its nearsightedness appearance of the SPR band ( $\sim 629$  nm).<sup>19,20</sup> Consequently, the substantial enhancement in the PL intensity may arise when the wavelength of the incident light or the PL are in the vicinity of the SPR wavelength.<sup>21</sup> The SPR driven excitation mechanism is responsible for intensified electromagnetic field around  $\text{Er}^{3+}$  ions that results an enhancement in  $\text{Er}^{3+}$  ions luminescence.<sup>20</sup> Meanwhile, quenching in emission intensity at higher NPs concentration<sup>22</sup> is ascribed to the re-absorption of SPR by NPs having plasmon absorption band range extended over the emission peak position of  $\text{Er}^{3+}$ .<sup>23</sup>



**Figure 4** (a) Excitation spectrum of the glass samples in range of 360 to 500 nm; (b) PL spectra for glass containing 0.2 mol% Au with Gaussian fit; (c) Luminescence spectra for all samples under 350 nm excitations; (d) PL enhancement factor showing enhancement and quenching ratio for respective glass samples with varying Au concentration

**Table 2** Au concentration dependent PL enhancement factor

Au concentration	Enhancement factor			
	468 nm	507 nm	554 nm	594 nm
0 mol%	1	1	1	1
0.2 mol%	15.46	16.80	18.35	20.23
0.4 mol%	10.38	11.38	12.88	14.97

Figure 5 depicts the schematics partial energy level diagram of Er<sup>3+</sup> in the vicinity of Au NPs embedded in the zinc sodium tellurite glass. The laser beam of 350 nm wavelength excites the Er<sup>3+</sup> ions to <sup>4</sup>G<sub>9/2</sub> excited states. The NR decays from <sup>4</sup>G<sub>9/2</sub> to <sup>4</sup>F<sub>5/2</sub> populate these levels which is responsible for generation of blue emission. Further, the NR decays takes place from <sup>4</sup>F<sub>5/2</sub> to <sup>4</sup>F<sub>7/2</sub> and <sup>4</sup>S<sub>3/2</sub>. The population of these levels is responsible for the origin of green emissions. In addition, the NR decays from <sup>4</sup>S<sub>3/2</sub> to <sup>4</sup>F<sub>9/2</sub> and the sequence population lead to the origin of orange emission. The observed emissions at 468, 507, 554 and 594 nm are primarily attributed to the combined mechanism of ground state absorption (GSA), energy transfer (ET) and co-operative energy transfer (CET) between two Er<sup>3+</sup> ions and the local field effects (LFE) due to Au NPs. Local field effect involves SPR excitation which is responsible for intensified electromagnetic field around Er<sup>3+</sup> ions results an enhancement in Er<sup>3+</sup> ions luminescence. The giant and highly localized electric field around the gold NPs may greatly enhance the transition yield of RE ions positioned in the proximity of Au NPs.<sup>22</sup>

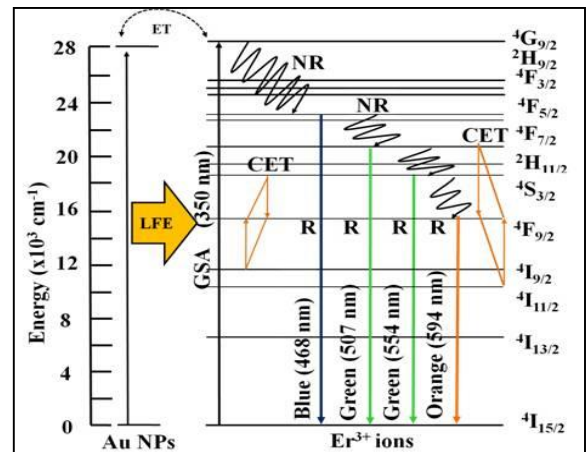


**Figure 5** Partial energy level diagram showing all emissions involving various mechanisms

### 4.0 CONCLUSION

We demonstrated the finely tuned spectroscopic properties of Au NPs embedded Er<sup>3+</sup> doped zinc sodium tellurite by varying the concentration of NPs. UV-Vis spectra of glass displayed the existence of six

absorption bands corresponding to 4f-4f transitions of Er<sup>3+</sup> ions. In addition, the manifestation of plasmon peak at around 629 nm is attributed to the presence of Au NPs. The distribution of Au NPs in the host matrix is confirmed via EDX analyses which revealed weak Au peak. The emission spectra of Er<sup>3+</sup> displayed a prominent peak at 594 nm. Further, glass containing 0.2 mol% Au exhibited a strong peak at 554 nm and 468 nm accompanied by a relatively moderate peak at 468 nm. The achieved significant enhancement in luminescence intensity in ratio of 20.23, 18.35, 16.80 and 15.46 is interpreted through the SPR mediated contribution of Au NPs during optical interaction. It is established that the remarkable augmentation in the spectroscopic response triggered by Au NPs mediated SPR effects may nominate these glasses as potential candidate for solid state lasers, color displays and versatile photonic devices.

### Acknowledgement

The authors wish to thank to UTM and Ministry of Higher Education (MoHE) for the financial support through GUP grant (Vote 05H36, 4F424 and 12H42). Asmahani is grateful to UMS for financial support through SGPUMS (Vote SGK0008-SG-2015) and RAG0067-SG-2015.

### References

- [1] Jlassi, I., Elhouichet, H., Hraiech, S. & Ferid, M. 2013. Effect of Heat Treatment on the Structural and Optical Properties of Tellurite Glasses Doped Erbium. *J. Lumin.* 132(3): 832-840.
- [2] Sahar, M. R., Jehbu, A. K. & Karim, M. M. 1997. TeO<sub>2</sub>-ZnO-ZnCl<sub>2</sub> Glasses for IR Transmission. *J. Non-Cryst. Solids.* 213-214: 164-167.
- [3] Sidek, H. A. A., Rosmawati, S., Talib, Z. A., Halimah, M. K. & Daud, W. M. 2009. Synthesis and Optical Properties of ZnO-TeO<sub>2</sub> Glass System. *J. Appl. Sci.* 6(8): 1489-1494.
- [4] de Almeida, R., da Silva, D. M., Kassab, L. R. P. & de Araujo, C. B. 2008. Eu<sup>3+</sup> Luminescence in Tellurite Glasses with Gold Nanostructures. *Opt. Commun.* 281(1): 108-112.
- [5] El-Mallawany, R. 1999. Tellurite glasses: Part 2. Anelastic, Phase Separation, Debye Temperature and Thermal Properties. *Mater. Chem. Phys.* 60(2):103-131.
- [6] Som, T. & Karmakar, B. 2009. Enhancement of Er<sup>3+</sup> Upconverted Luminescence in Er<sup>3+</sup>: Au-Antimony Glass Dichroic Nanocomposites Containing Hexagonal Au Nanoparticles. *Opt. Soc. Am. B.* 26(12): B21-B27.
- [7] Jlassi, I., Elhouichet, H. & Ferid, M. 2011. Thermal and Optical Properties of Tellurite Glasses Doped Erbium. *J. Mater Sci.* 46(3): 806-812.
- [8] Rivera, V. A. G., Ledemi, Y., Osorio, S. P. A., Manzani, D., Messaddeq, Y., Nunes, L. A. O. & Marega Jr. E. 2012. Efficient Plasmonic Coupling between Er<sup>3+</sup>:(Ag/Au) in Tellurite Glasses. *J. Non-Cryst. Solids.* 358(2): 399-405.
- [9] Kassab, L. R. P., Camilo, M. E., Amancio, C. T., da Silva, D. M. & Martinelli, J. R. 2011. Effects of Gold Nanoparticles in the Green and Red Emissions of TeO<sub>2</sub>-PbO-GeO<sub>2</sub> Glasses Doped with Er<sup>3+</sup>-Yb<sup>3+</sup>. *Opt. Mater.* 33(12): 1948-1951.
- [10] Selvaraju, K. & Marimuthu, K. 2013. Structural and Spectroscopic Studies on Concentration Dependent Sm<sup>3+</sup> Doped Boro-Tellurite Glasses. *J. Alloy Compd.* 553: 273-281.
- [11] Dimitrova, M. T., Ivanova, Y. Y., Dimitriev, Y. B., Salvado, I. M. M. & Fernandes, M. H. F. V. 2013. Nanostructured Float-Glasses After Ion-Exchange in Melts Containing Silver or Copper Ions. *Int. J. Mat. Chem.* 3: 29-38.
- [12] Jlassi, I., Elhouichet, H., Hraiech, S. & Ferid, M. 2012. Effect of Heat Treatment on the Structural and Optical Properties of Tellurite Glasses Doped Erbium. *J. Lumin.* 132(3): 832-840.
- [13] Malta, O. L., Santa-Cruz, P. A., de Sa, G. F. & Auzel, F. 1985. Fluorescence Enhancement Induced by the Presence of Small Silver Particles in Eu<sup>3+</sup> Doped Materials. *J. Lumin.* 33(3): 261-272.
- [14] Puchalski, M., Dabrowski, P., Olejniczak, W., Krukowski, Kowalczyk, P. & Polanski, P. K. 2007. The Study of Silver Nanoparticles by Scanning Electron Microscopy, Energy Dispersive X-ray Analysis and Scanning Tunneling Microscopy. *J. Mat. Sci.* 25(2): 473-478.
- [15] Jusman, Y., Ng, S. C. & Osman, N. A. A. 2014. Investigation of CPD and HMDS Sample Preparation Techniques for Cervical Cells in Developing Computer-Aided Screening System Based on FE-SEM/EDX. *Scientific World J.* Doi: 10.1155/2014/289817.
- [16] Obadina, V. O. & Reddy, B. R. 2013. Investigation of Silver Nanostructures and Their Influence on the Fluorescence Spectrum of Erbium-Doped Glasses. *Optics Photon.* 3: 45-50.
- [17] Selvaraju, K. & Marimuthu, K. 2012. Structural and Spectroscopic Studies on Concentration Dependent Er<sup>3+</sup> Doped Boro-Tellurite Glasses. *J. Lumin.* 132(5): 1171-1178.
- [18] Sharma, Y. K., Surana, S. S. L., Singh, R. K. & Dubedi, R. P. 2007. Spectral Studies of Erbium Doped Soda Lime Silicate Glasses in Visible and Near Infrared Regions. *Opt. Mater.* 29(6): 598-604.
- [19] da Silva, D. M., Kassab, L. R. P., Luthi, S. R., de Araujo, C. B., Gomes, A. S. & Bell, M. J. V. 2007. Frequency Upconversion in Er<sup>3+</sup> Doped PbO-GeO<sub>2</sub> Glasses Containing Metallic Nanoparticles. *Appl. Phys. Lett.* 90: 081913.
- [20] Pan, Z., Ueda, A., Aga Jr. R., Burger, A., Mu, R. & Morgan, S. H. 2010. Spectroscopic Studies of Er<sup>3+</sup> Doped Ge-Ga-S Glass Containing Silver Nanoparticles. *J. Non-Cryst. Solids.* 356(23-24): 1097-1101.
- [21] de Araujo, C. B., da Silva, D. S., Assumpcao, T. A. A., Kassab, L. R. P. & da Silva, D. M. 2013. Enhanced Optical Properties of Germanate and Tellurite Glasses Containing Metal or Semiconductor Nanoparticles. *Scientific World J.* doi:10.1155/2013/385193.
- [22] Som, T. & Karmakar, B. 2009. Nanosilver Enhanced Upconversion Fluorescence of Erbium Ions in Er<sup>3+</sup>: Ag-Antimony Glass Nanocomposites. *J. Appl. Phys.* 105: 013102.
- [23] Amjad, R. J., Sahar, M. R., Dousti, M. R., Ghoshal, S. K. & Jamaludin, M. N. A. 2013. Surface Enhanced Raman scattering and Plasmon Enhanced Fluorescence in Zinc-Tellurite Glass. *Opt. Express.* 21: 14282-14290.